The Cosmic Background
Radiation 25 Years Later
L'Aquila, Italy
June 1989

MEDIUM SCALE MEASUREMENTS OF THE COSMIC MICROWAVE BACKGROUND AT 3.3 mm

Philip M. Lubin
Peter R. Meinhold †
Alfredo O. Chingcuanco ‡

Physics Department
University of California
Santa Barbara, CA 93106

We have developed a system for making measurements of spatial fluctuations in the Cosmic Microwave Background Radiation at 3 mm wavelength, on an angular scale of .5 to 5 degrees. The system includes a telescope with a Gaussian beam with full width at half maximum (FWHM) of 20 to 50 arc-minutes, a Superconductor-Insulator-Superconductor (SIS) coherent receiver operating at 90 GHz, and for balloon flights, a pointing system capable of 1 arc-minute RMS stabilization. We report on results from the first flight of the stabilized platform, as well as results from ground based measurements made from the South Pole station in December, 1988.

INTRODUCTION

Searches for structure in the spatial distribution of the Cosmic Background Radiation (CBR) are one of the few experimental tests of cosmological models. Currently no definitive detections of anisotropy have been made except for the dipole term, and limits of 20 to 200 parts per million have been established from 10 arc-seconds to 90 degrees angular scale (see figure 1). In the region from 1 to 10 degrees few experiments have been done with sufficient sensitivity to seriously constrain cosmological models, galaxy formation scenarios in particular. Recent reports of detection in this region are suggestive but may suffer from systematic and galactic emission subtraction problems.

At the largest scale (180 degrees) measurements of the doppler shift dipole anisotropy produced by our peculiar motion relative to the frame of the CBR are

---

† also, Physics Dept., UC Berkeley
‡ also, M.E. Dept., UC Berkeley

limited not by statistics but by calibration errors and galactic contamination. Measurements at this scale have also been used to place upper limits at angular scales down to about 10 degrees. (Strukov et al., (1988)) To date, all measurements on these scales (greater than about 10-20 degrees) have been done from space or high altitude balloon payloads in order to avoid contributions due to atmospheric fluctuations at large angles. Because of the large solid angle of these measurements, point source contamination is generally not a problem, whereas diffuse galactic emission from Bremsstrahlung, synchrotron, and dust are, in addition to off axis sidelobe contamination by the earth, sun, and moon.

Measurements on very small angular scales (arc-seconds to a few arc-minutes) have been performed from large, ground based, single dish and synthesized aperture telescopes. For these scales, source confusion begins to be a problem at the $\frac{\Delta T}{T} \sim 10^{-5} - 10^{-6}$ level (Franchesini et al., (1988)). In addition, current ideas about the generation of structure in the CBR include smoothing on scales of order 10 arc-minutes due to the finite "thickness" of the surface of last scattering. This tends to lower the level at which upper limits on $\frac{\Delta T}{T}$ put constraints on theories of galaxy evolution.

The Sachs-Wolfe (SW) effect (Sachs, Wolfe, (1967)), gravitational doppler shifting of photons moving through evolving gravitational potentials, is the primary theoretical mechanism for temperature fluctuations at angular scales greater than a few degrees. The most sensitive tests for theories of galaxy evolution are expected to be on scales of about 1 degree, above the scale where recombination and reheating effects are important, and below that where correlations due to the Sachs Wolfe effect begin to dominate. Some Cold Dark Matter scenarios for galaxy formation predict $\frac{\Delta T}{T}$ on .5 to 5 degree scales to be larger than the SW fluctuations at larger angles (Vittorio et al.(1988)). For these reasons, interest in experiments in the .5 to 10 degree range has risen in the past few years. The two primary systematic difficulties with doing sensitive experiments in this angular range are the atmosphere, which has time varying structure, and galactic dust contamination, which must be modelled and possibly subtracted.

Our Experiment

We have chosen to work at 3 mm, where emission from the galaxy is low. Figure 2 shows the pole value of a cosecant fit in galactic coordinates, to several different large scale data sets, as a function of frequency. The plot shows that 3 mm is near the minimum.

While this choice of frequency reduces the problem of galactic contamination, problems with atmospheric emission are increased. Figure 3 shows the antenna temperature due to the atmosphere as a function of frequency at sea level, 3.6 km, and balloon altitudes. The plot is based on an atmospheric model with a standard temperature and pressure versus altitude profile, using water, oxygen and ozone absorption lines. It is evident that in order to work at 3 mm, one requires either a very stable atmosphere or a high enough altitude that the emission lines are not saturated and the measurement can be done between molecular transitions. For example, at sea level, the atmospheric emission is more than 6 orders of magnitude higher than a desired sensitivity of $\frac{\Delta T}{T} = 10^{-5}$.

We have built a system to make measurements on .5 to 5 degree scales, and have carried out experiments at balloon altitude and at the South Pole Station. Our gondola flew at about 30 km, where the precipitable water is approximately 3 x 10^{-4} mm. We chose the South Pole as a ground observation site because of the

low water content and previously reported high stability of the atmosphere there. Figure 4 shows precipitable water for the time we were observing. Following is a brief description of the balloon payload, flight performance, and details of the South Pole expedition and results.

Balloon Payload

In order to get useful integration time, we need a balloon gondola capable of stabilizing to a fraction of a beam width, which is 15 arc-minutes for our system. This requires an active stabilization system and some absolute pointing reference. Figures 5 and 6 show a diagram and schematic for our pointing platform. The primary elements in the pointing system are: an inertial guidance system consisting of 3 axis gyros, accelerometers, and a navigation processor; a CCD Star camera, for real time verification of absolute pointing accuracy and stability performance; A reaction wheel for azimuth angle stabilization and control; and an active triple race bearing system which serves to decouple the rotations of the balloon from the gondola, in addition to providing a controlled way to dump angular momentum accumulated in the reaction wheel from external perturbations on the gondola. The servo control and data taking are implemented with an on-board computer, with real-time interaction via telemetry from the ground. This package was first flown from the National Scientific Balloon Facility in August, 1988.

Optical System

Our optical system is an off axis Gregorian telescope, consisting of a 6.5 degree (FWHM) corrugated scalar feed, a 1 meter diameter, 1 meter focal length primary, with a confocal elliptical secondary mirror. The resulting beam can have a FWHM of 20 to 50 arc-minutes, depending on the secondary mirror used (our results are for a FWHM of 36 arc-minutes). Rotation of the secondary about the axis of the feed horn throws the beam horizontally on the sky. We chop the beam by a physical angle of 1 degree on the sky at 10 Hz to make a first difference measurement of temperature fluctuations. Our primary reason for using this configuration is the very low sidelobe response of such an antenna. For the central lobe, the beam is well approximated by a Gaussian of $\sigma = 15$ arc-minutes. $P(\Omega) = e^{-\theta^2/2\sigma^2}$ With a FWHM of 36 arc-minutes, the ratio of solid angle available for contamination to that in the beam puts stringent limits on the allowable sidelobe response. We measured our sidelobes down to -85 dB, without ground shields. In addition a ground shield was attached during data taking both during the balloon flight and at the South Pole.

SIS Receiver

A schematic of our detection system is shown in figure 7. We use a Niobium SIS (Superconductor-Insulator-Superconductor) based coherent radiometer, operating at 90 GHz. Our mixer, HEMT IF amplifier (spot noise about 1 K), and cooled RF section enable us to achieve a system spot noise of about 33 Kelvin at a mixer physical temperature of 3.5 Kelvin. Receiver performance is shown in figure 7. During data taking at the South Pole, our full band (0.6 GHz) noise was approximately 40 K, providing a theoretical system sensitivity (before chopping) of $\Delta T = 1.6 \frac{mK}{\sqrt{Hz}}$.

Flight Results

Our flight from Palestine Texas in August, 1988 was a highly successful test

of the stabilization and detector systems. The package got about eight hours at a float altitude between 95,000 and 100,000 ft., with no major damage on landing. The gondola achieved a pointing stability better than 1 arc-minute (RMS), and we were able to perform several important system tests during the flight.

Figure 8 shows actual azimuth angle as a function of time, showing our three point scan trajectory superimposed on the tracking for an az-el mount. Figure 9 is a calibration scan of Jupiter done during flight as a check of calibration factor and beam profile. Figure 10 shows a real-time scan of the galactic center, which we use to scale IRAS 100 micron data to our frequency for subtraction (this is discussed in detail later in this work). Unfortunately, a telemetry problem prevented us from obtaining enough integration time to get useful data on CBR fluctuations.

South Pole Results

From late November, 1988 to early January, 1989, we made measurements of CBR fluctuations and galactic emission from the South Pole station, replacing the azimuth stabilization with a servoed rotation table. Figure 11 shows a calibration scan of the moon, along with an approximate theoretical curve, based on a model for moon emission as a function of moon phase.

Since galactic dust emission is a probable cause of error, we need to determine the scaling between short wavelength data to 3 mm. Comparing a simple cosecant fit to the IRAS 100 micron data and the cosecant amplitude for 90 GHz from our earlier large scale anisotropy flights (see figure 2) gives approximately 10 $\frac{\mu K}{MJy/Sr}$, which is consistent with the number obtained by comparing the IRAS data to the flight scan of the galactic center. Figure 12 shows our South Pole plane crossing scan with error bars, as well as a first difference scan of the IRAS 100 micron map, scaled by the above number. Since these three comparisons are consistent, we can estimate the contribution of dust emission to our data. We implicitly must assume here that the dust emissivity scaling is the same over the sky. We chose to measure in a region around RA=21.5, DEC=-73 ($l^{II} = -40.6, b^{II} = -37.43$), where the IRAS 100 micron map shows a total intensity minimum of about 4-10 MJy/Sr, and first differences only of order 1-2 MJy/Sr (see figure 13a,b). Using the galaxy data described above, this would be about 10-20 microKelvins in our first difference data, which is small though not completely negligible compared to our errors (about 40 to 60 microKelvin per data point). Figure 13 shows two views of the IRAS 100 micron data in celestial coordinates, with an expanded view of the measurement region.

The total dust intensity contribution in this region of 4-10 MJy/Sr could then be about 40 to 100 microKelvins, clearly of concern for future measurements. We are currently at the point in sensitivity where even in the best parts of the sky, dust emission at 3 mm wavelength is predicted to be near our detection limit. To do an order of magnitude more sensitive measurement will almost certainly require galactic subtraction preferably by multiple wavelength measurements.

CBR Data

We observed 9 points with 1 degree physical chop angle on the sky, in a strip, spaced so that one beam from each point coincided with one beam from the next point. Several strips were measured to different sensitivities. This gives us a powerful test for systematic errors, as well as providing information on a variety of angular scales, from the beam sigma of 15 arc-minutes up to approximately 5 degrees. After time lost due to setting up, equipment problems and bad weather,

we obtained about 80 hours of data, which reduced to about 70 hours after editing out radio interference and bad sky data. Our scan system gave us an efficiency (time spent on the measurement points) of only 60 percent, reducing the real data further to about 43 hours.

With a calculated statistical system sensitivity (on the sky) of 3 $\frac{mK}{\sqrt{Hz}}$, or 4 $\frac{mK}{\sqrt{Hz}}$ with sky shot noise included, we measured approximately 6 $\frac{mK}{\sqrt{Hz}}$ (RMS) on the sky for short time scales. Figure 14 is a histogram of the RMS in 100 second bins, showing the stability of the short term sky noise over time (for 'good' days). Several runs were made of just atmospheric noise and are being investigated to help understand the nature of the sky noise.

Raw Data Fitting

In order to work with the data, we have found it necessary to remove slow drifts in offset, which can be attributed to long term sky variations, changing electrical offsets, and temperature gradients on the primary. Our observing technique allows a natural way to remove such non- intrinsic shifts. Since we scan from one side of the strip to the other and then back in a period of about 30 minutes, linear variations on time scales long compared to 30 minutes can be removed without removing CBR structure. The results plotted in figure 15 are the summed data for each point, with statistical error bars, where the raw data have been edited and piecewise linear fit in time, over times of approximately 3 hours. The results for a truncated Fourier fit subtraction, constructed to fit only structure longer than 3 scans, as well as a Legendre polynomial fit, are consistent with the linear fit presented. The error bars on this data set are consistent with the short term RMS fluctuations.

Data Analysis

Looking at the data set in figure 15, a linear trend is evident across the points. Although this could be taken as an indication of intrinsic structure in the background radiation, we are unwilling to rule out some systematic effect to produce this. As an example, the sun was at RA of about 18 hours during our data taking, and contributions from this on the 100 μK level are not out of the question. We choose to remove the linear component from the data and consider the result to be our final set, which is shown in figure 16. This set with error bars shown has a reduced chisquare of 1.53, corresponding to approximately 20 percent probability of being consistent with the null hypothesis. We are currently analyzing the data to test for various cosmological models, such as the cold dark matter galaxy formation model, scale invariant Gaussian fluctuations, etc.. These calculations will be presented in a forthcoming paper.

3. CONCLUSIONS

Acknowledgements

This work was supported by the National Aeronautics and Space Administration, the National Science Foundation, California Space Institute, the University of California, and the U.S. Army. This work would not have been possible without the support and encouragement of Nancy Boggess, Buford Price, and John Lynch. We wish to especially thank Anthony Kerr and S.K. Pan of NRAO for supplying the exceptional SIS mixer. The Nb/$Al-Al_2O_3$/Nb junctions used were supplied by

Hypres Corporation. Special thanks to Robert Wilson, Anthony Stark, Joe Stack, and Paul Moyer at Bell Labs for assistance in machining the primary and secondary mirrors. We gratefully acknowledge the support of Donald Morris. In particular we would like to thank Bill Coughran, and rest of the South Pole ANS support staff for the 1988-89 polar summer.

4. REFERENCES

R.D. Davies, A.N. Lasenby, R.A. Watson, E.J. Daintree, J. Hopkins, J. Beckman, J. Sanches-Almeida, and R. Rebolo, *Nature*, **326**, 462, (1987).

E.B. Fomalont, K.I. Kellerman, M.C. Anderson, D. Weistrop, J.V. Wall, R.A. Windhorst, and J.A. Kristian, *Ap. J.*, submitted (1988).

A.N. Lasenby, Ph.d. Thesis (1981).

F. Melchiorri, B.O. Melchiorri, C. Ceccarelli, and L. Pietranera, *Ap. J.*, **250**, L1, (1981).

S.K. Pan, M.J. Feldman, A.R. Kerr, and P. Timbie, *Applied Physics Letters*, **43**. 8, (1983).

A.C.S. Readhead, C.R. Lawrence, S.T. Myers, W.L.W. Sargent, H.E. Hardebeck, and A.T. Moffet, *Ap. J.*, submitted (1989).

R. Sachs and A. Wolfe, *Ap. J.*, **147**, 73, (1967).

I.A. Strukov, D.P. Skulachev, A.A. Klypin, *Large Scale Structure of the Universe*, J. Audouze, et al (eds.), IAU #130.

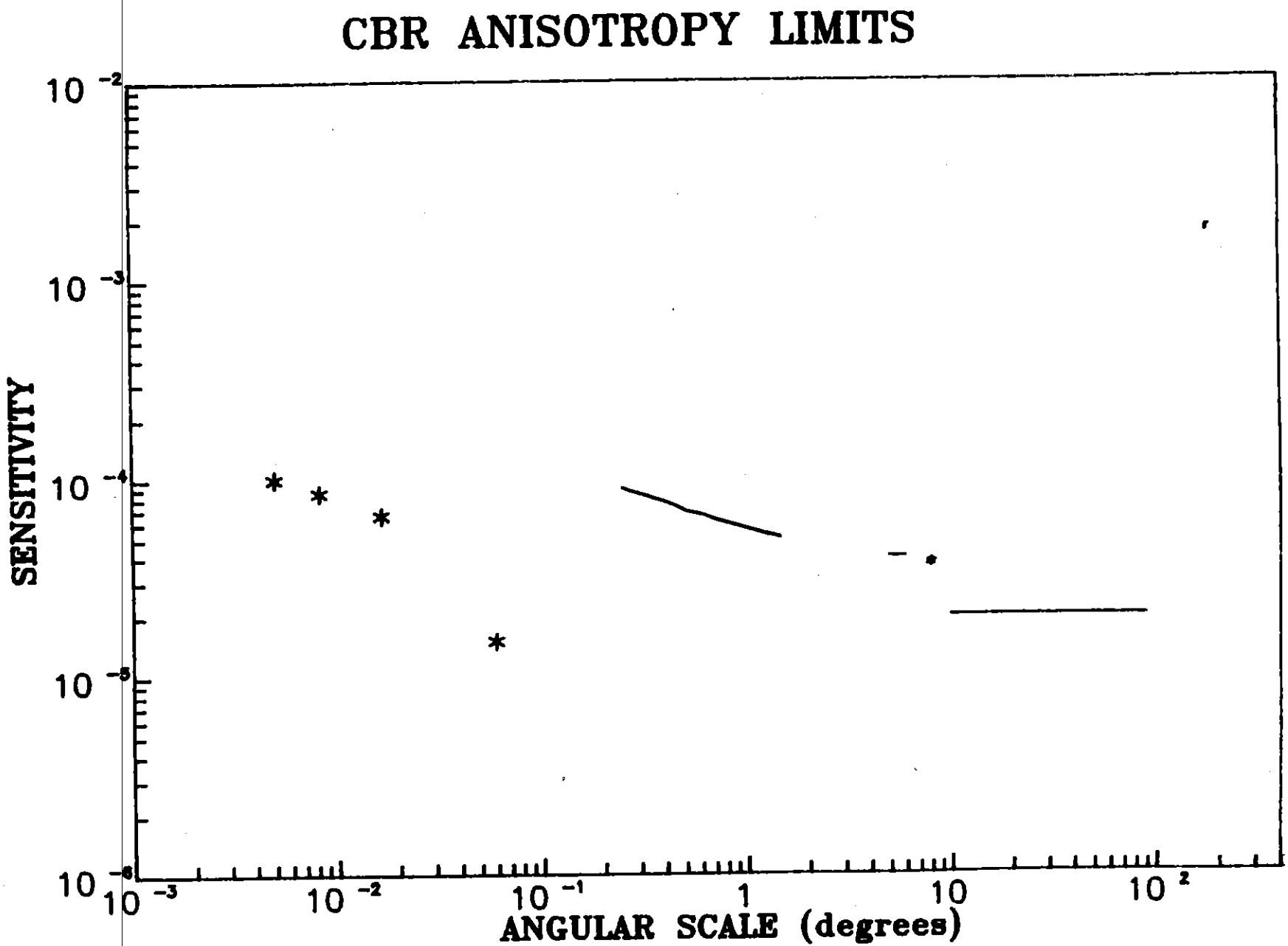
CBR ANISOTROPY LIMITS
SENSITIVITY
10 -2
10 -3
10 -4
10 -5
10 -6
10 -3
10 -2
10 -1
1
10
10 2
ANGULAR SCALE (degrees)

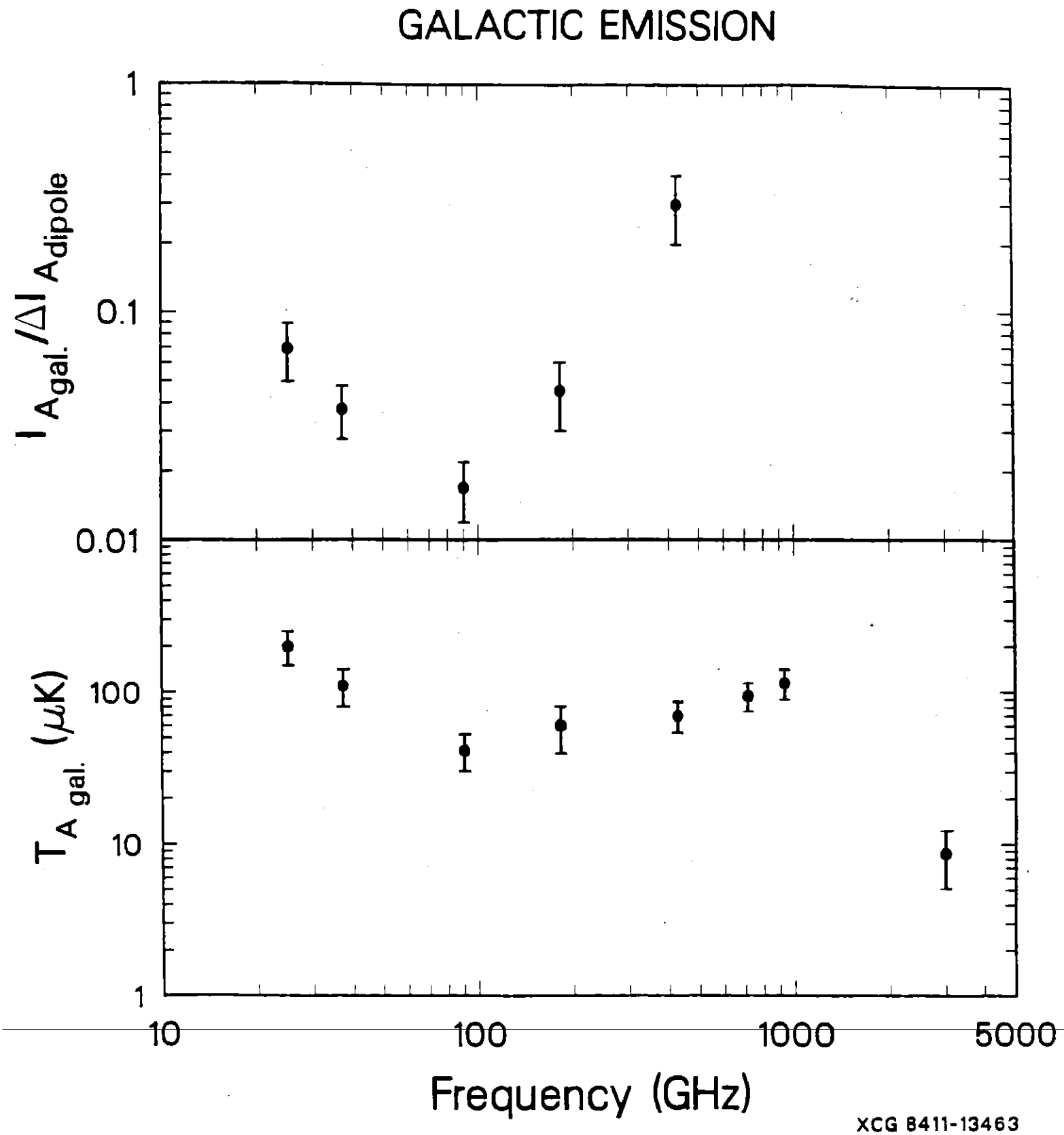
GALACTIC EMISSION
1
0.1
0.01
$I_{A_{gal.}}/\Delta I_{A_{dipole}}$
100
10
1
$T_{A\ gal.}$ (μK)
10
100
1000
5000
Frequency (GHz)
XCG 8411-13463

ATMOSPHERIC EMISSION AT 0, 3.6 AND 30 KM

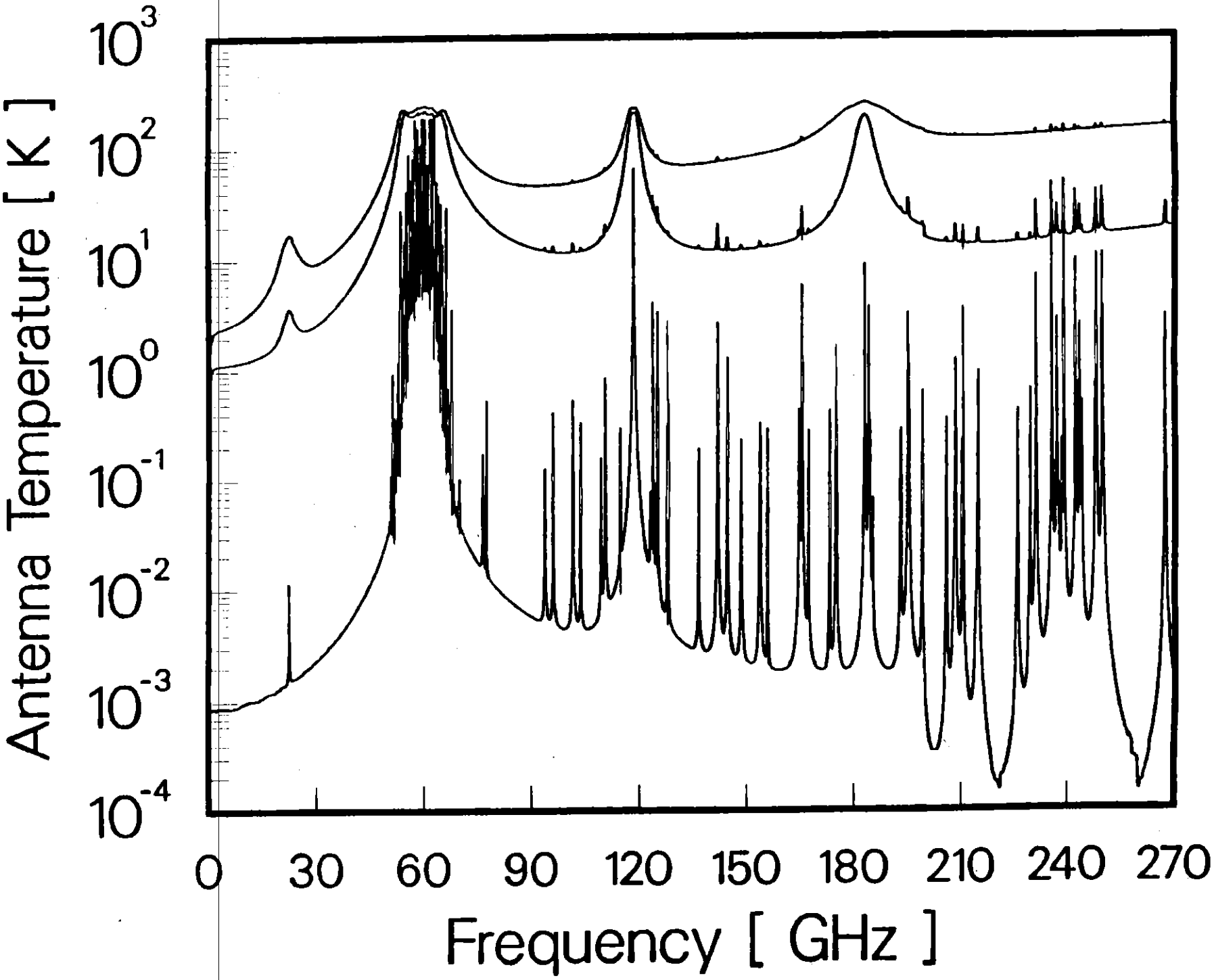

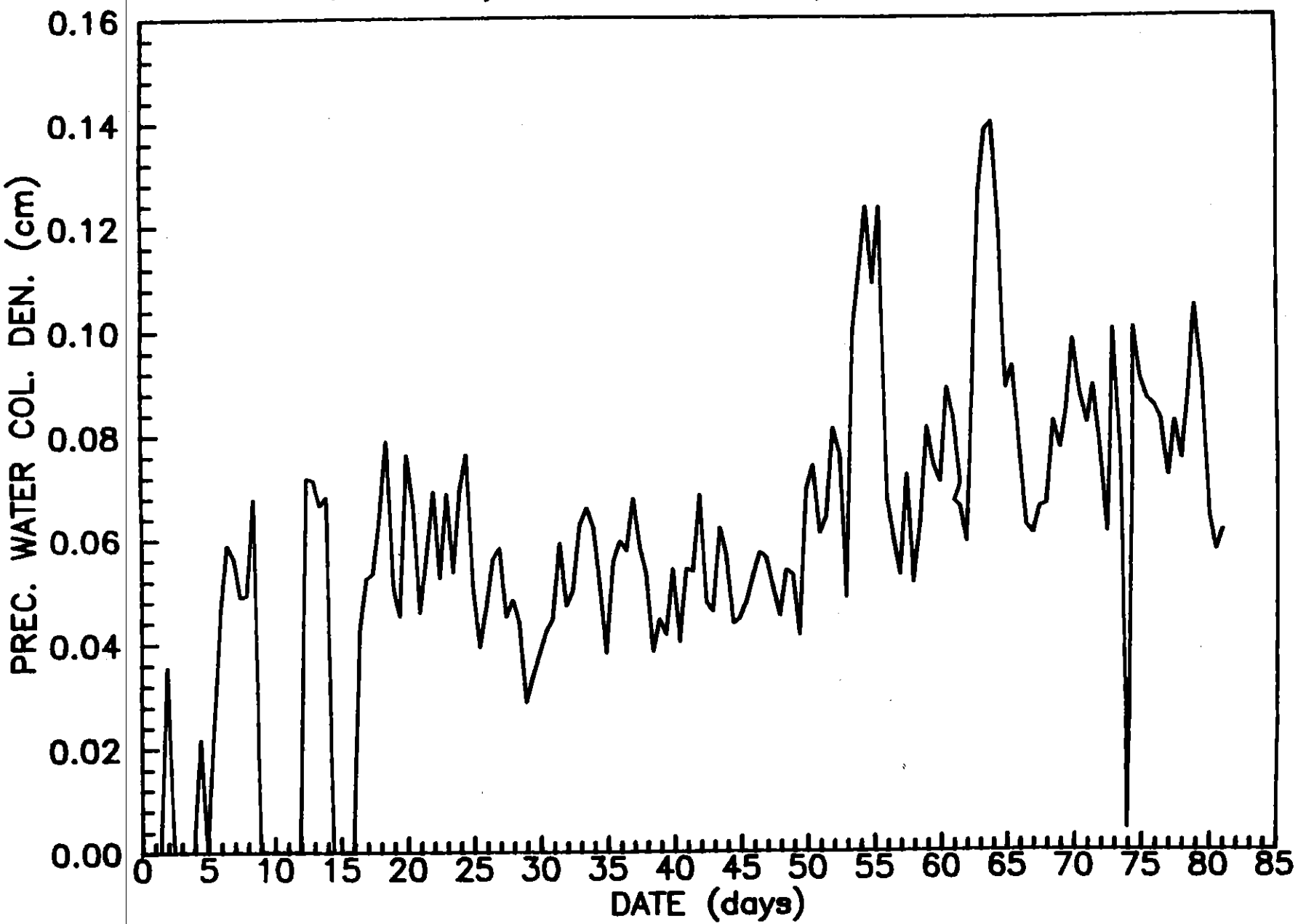
SOUTH POLE PRECIPITABLE WATER COLUMN DENSITY
NOVEMBER, 1988 TO JANUARY, 1989
PREC. WATER COL. DEN. (cm)
0.16
0.14
0.12
0.10
0.08
0.06
0.04
0.02
0.00
0 5 10 15 20 25 30 35 40 45 50 55 60 65 70 75 80 85
DATE (days)

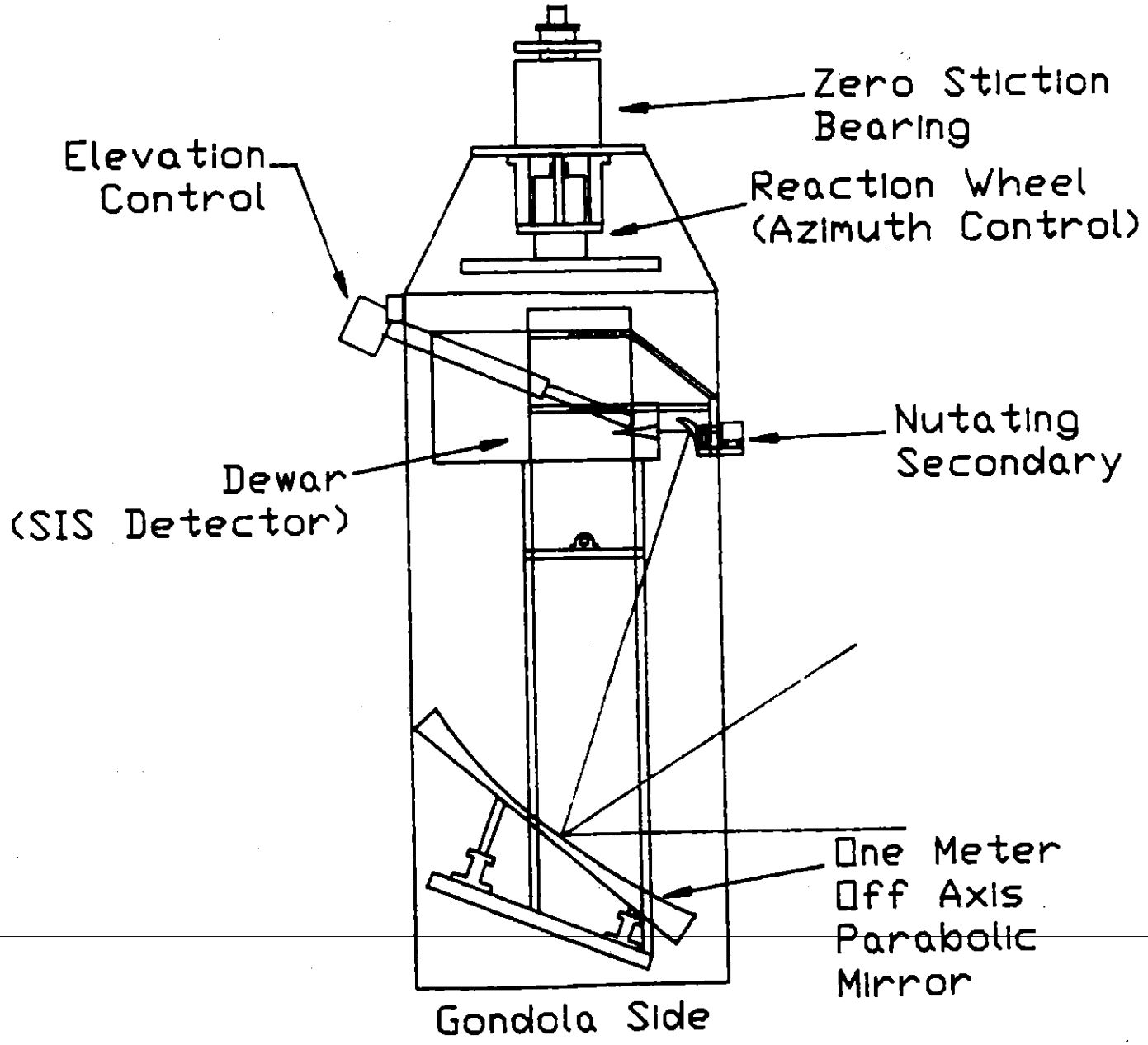
Zero Stiction
Bearing
Elevation
Control
Reaction Wheel
(Azimuth Control)
Nutating
Secondary
Dewar
(SIS Detector)
One Meter
Off Axis
Parabolic
Mirror
Gondola Side

Pointing Control System

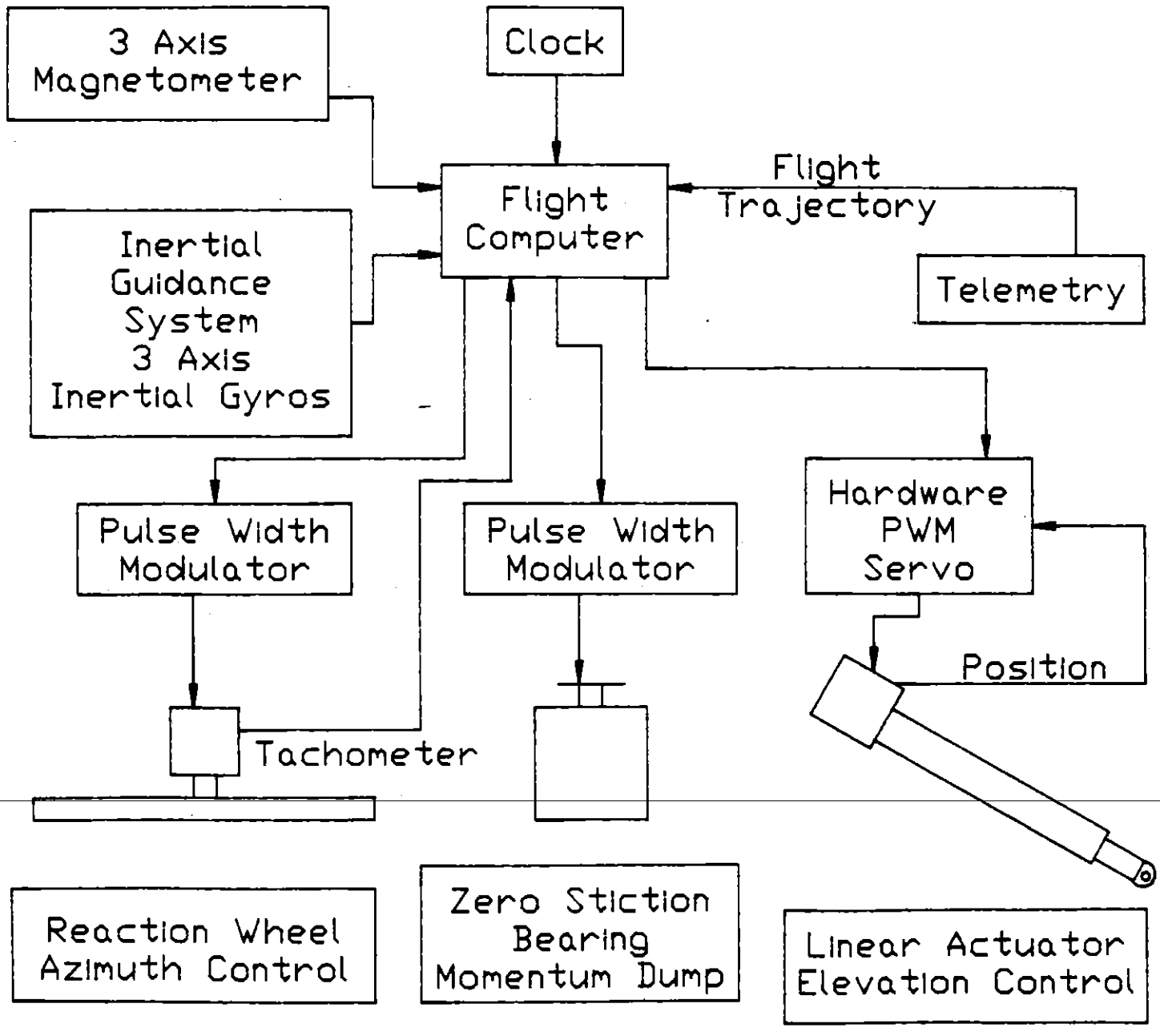

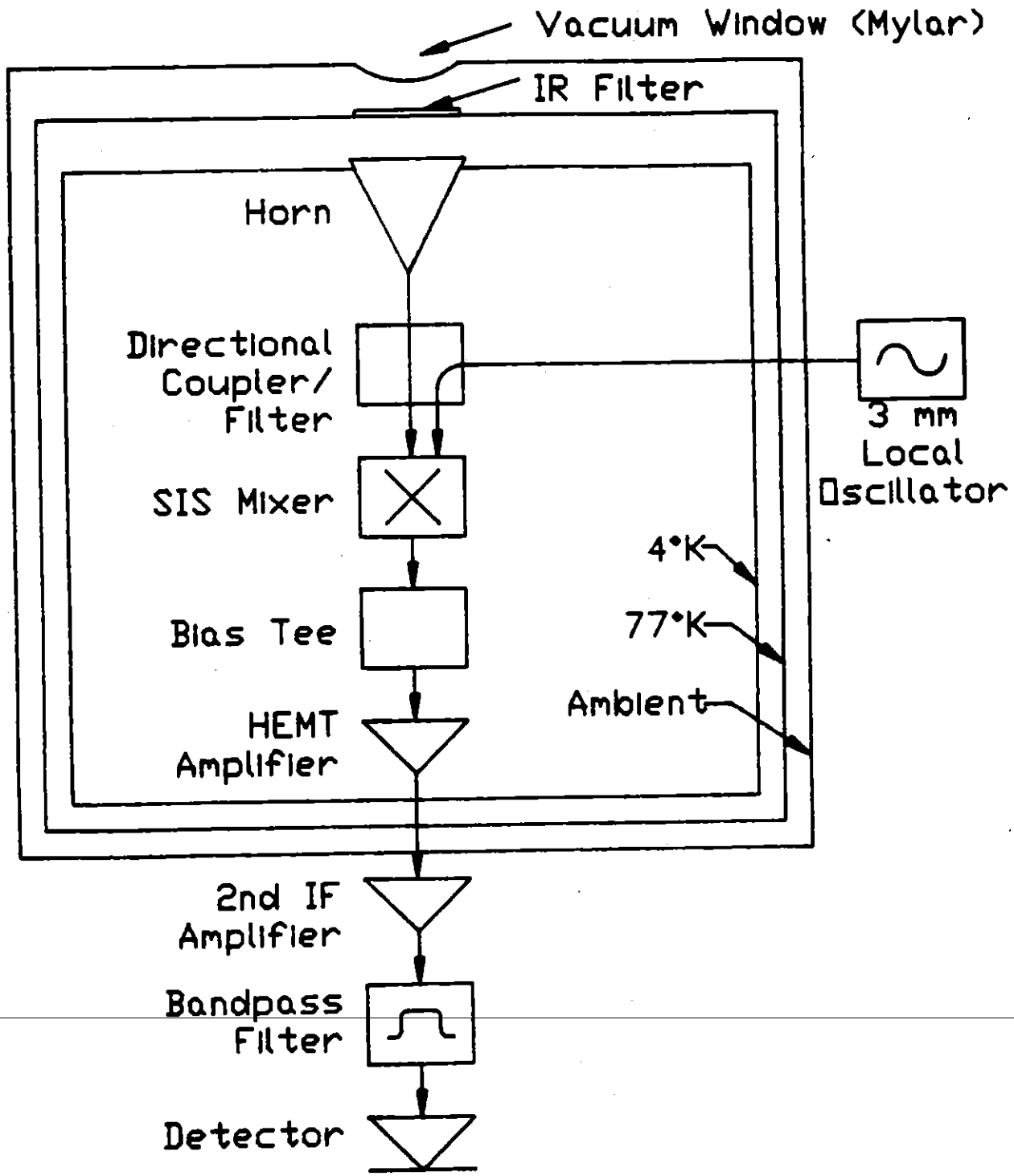
Vacuum Window (Mylar)
IR Filter
Horn
Directional Coupler/ Filter
3 mm Local Oscillator
SIS Mixer
4°K
77°K
Ambient
Bias Tee
HEMT Amplifier
2nd IF Amplifier
Bandpass Filter
Detector

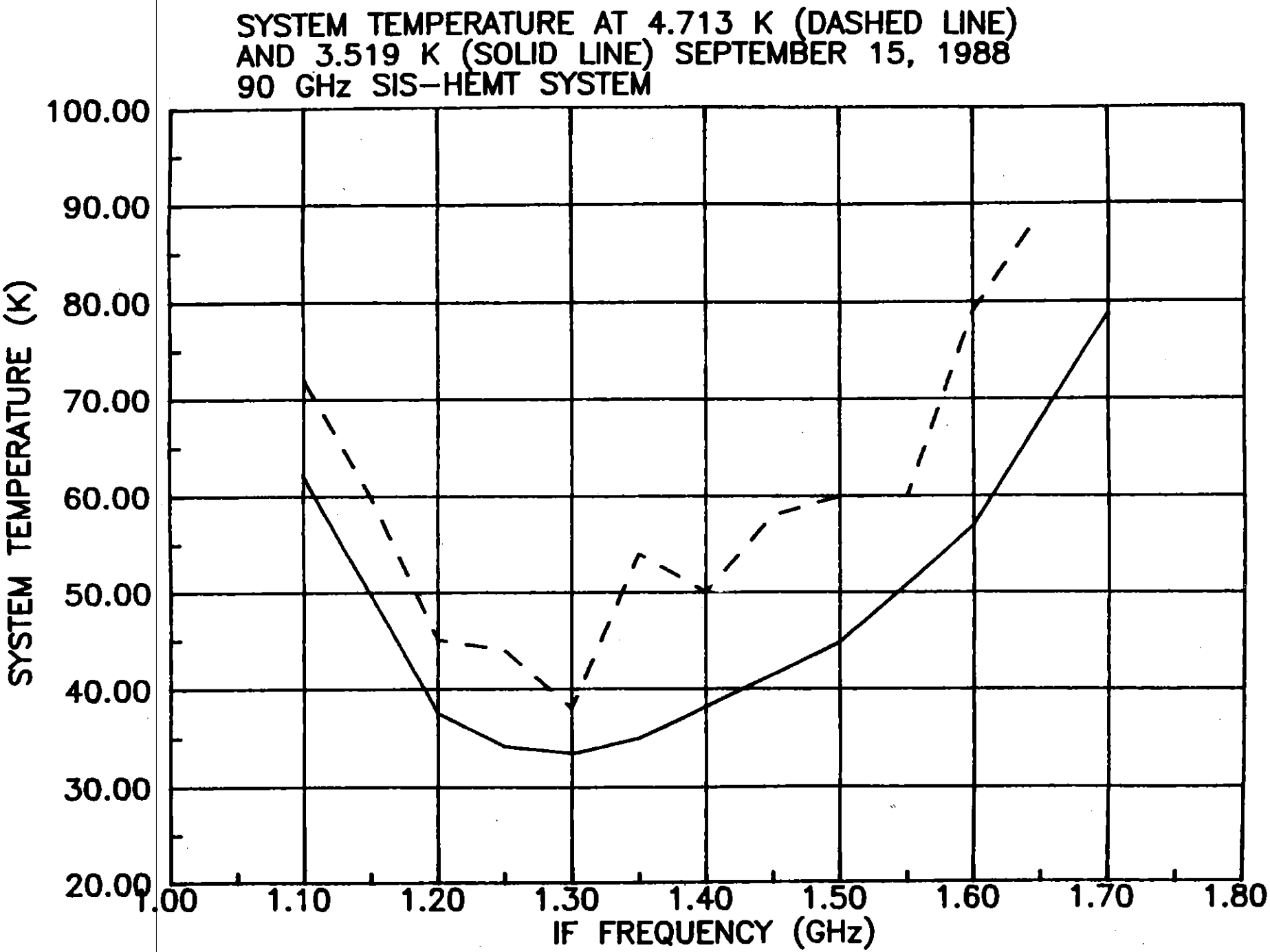
SYSTEM TEMPERATURE AT 4.713 K (DASHED LINE)
AND 3.519 K (SOLID LINE) SEPTEMBER 15, 1988
90 GHz SIS-HEMT SYSTEM
SYSTEM TEMPERATURE (K)
100.00
90.00
80.00
70.00
60.00
50.00
40.00
30.00
20.00
1.00
1.10
1.20
1.30
1.40
1.50
1.60
1.70
1.80
IF FREQUENCY (GHz)

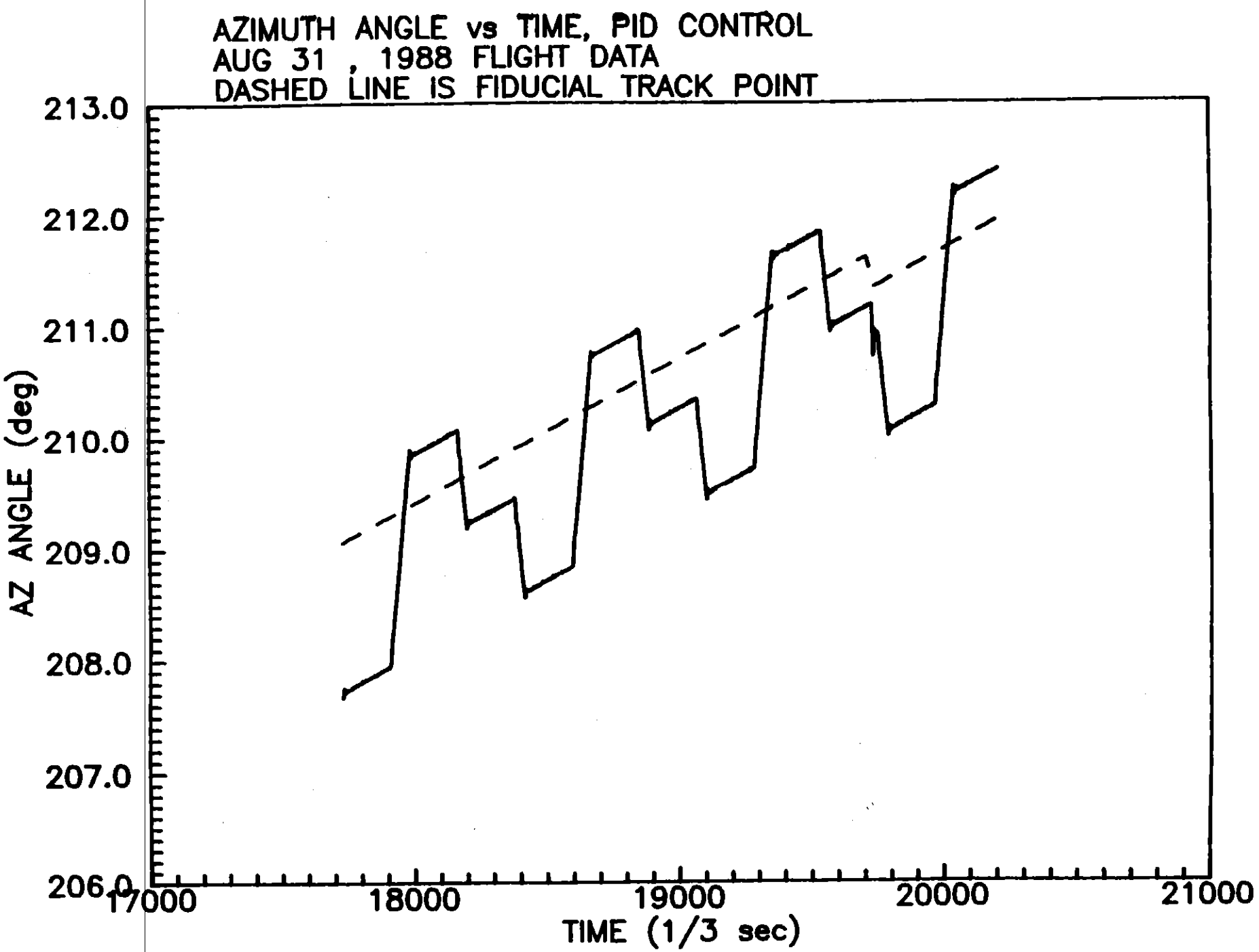
AZIMUTH ANGLE vs TIME, PID CONTROL
AUG 31 , 1988 FLIGHT DATA
DASHED LINE IS FIDUCIAL TRACK POINT
213.0
212.0
211.0
210.0
209.0
208.0
207.0
206.0
AZ ANGLE (deg)
17000
18000
19000
20000
21000
TIME (1/3 sec)

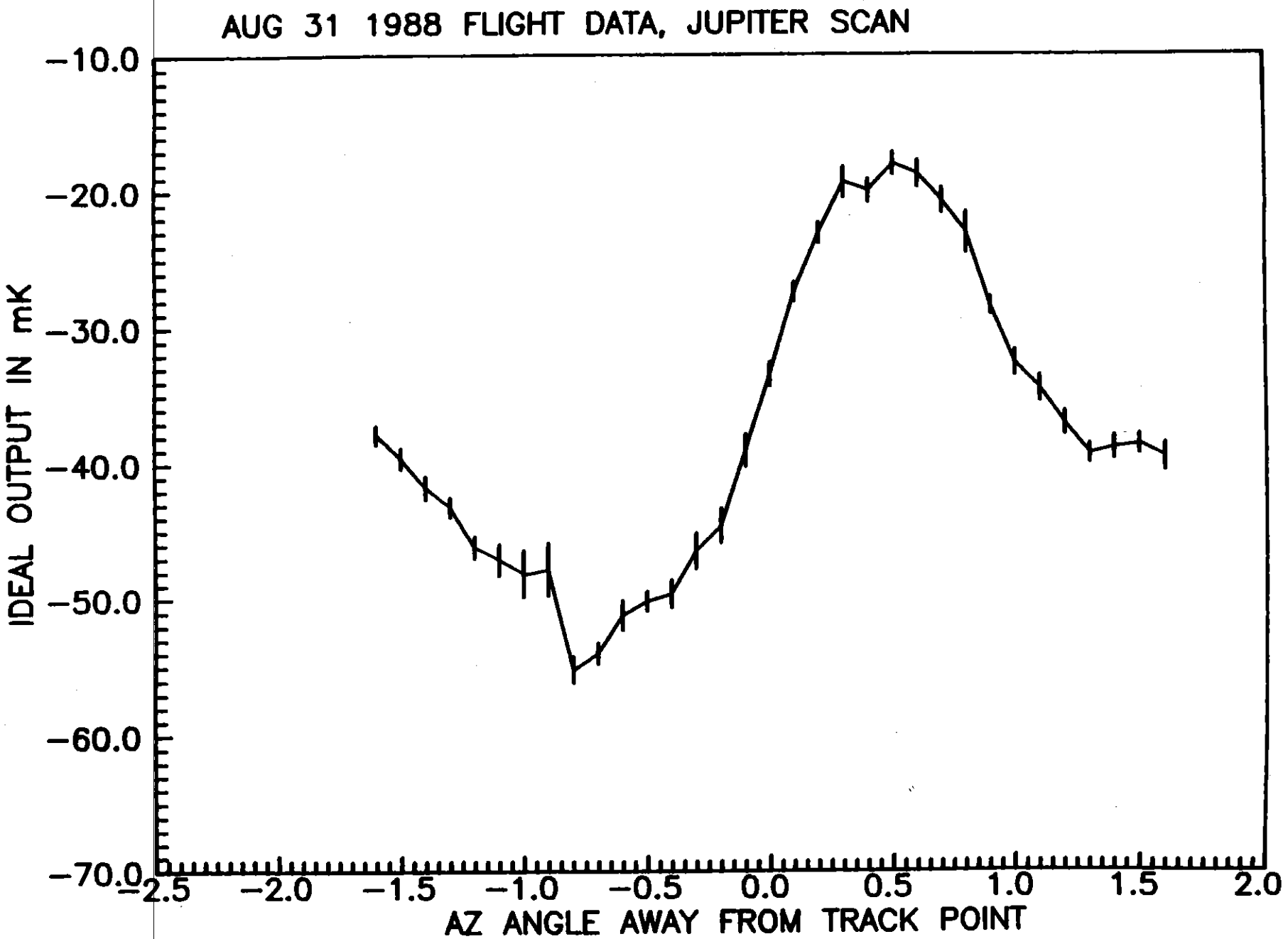
AUG 31 1988 FLIGHT DATA, JUPITER SCAN
IDEAL OUTPUT IN mK
-10.0
-20.0
-30.0
-40.0
-50.0
-60.0
-70.0
-2.5
-2.0
-1.5
-1.0
-0.5
0.0
0.5
1.0
1.5
2.0
AZ ANGLE AWAY FROM TRACK POINT

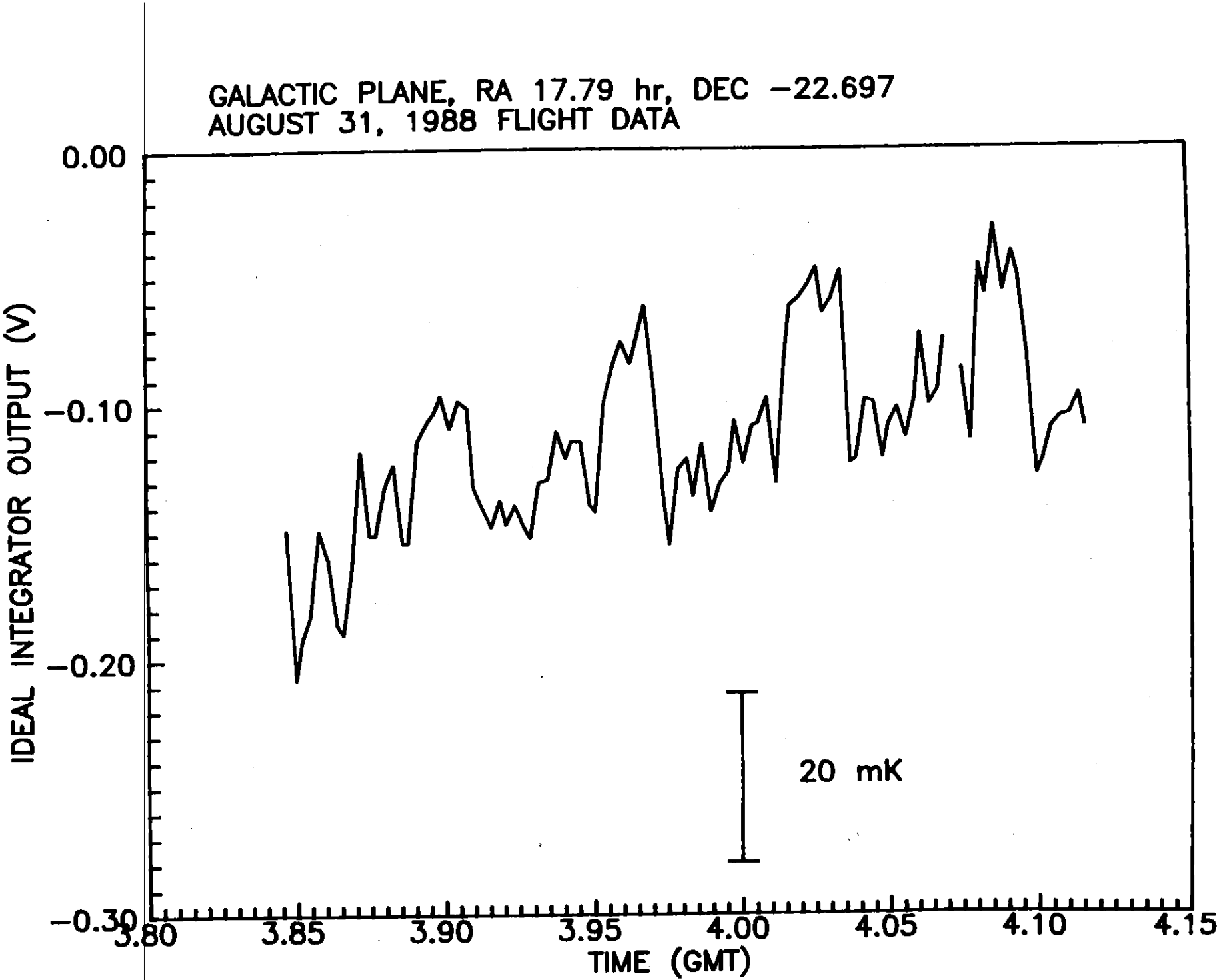
GALACTIC PLANE, RA 17.79 hr, DEC −22.697
AUGUST 31, 1988 FLIGHT DATA
0.00
−0.10
−0.20
−0.30
IDEAL INTEGRATOR OUTPUT (V)
20 mK
3.80
3.85
3.90
3.95
4.00
4.05
4.10
4.15
TIME (GMT)

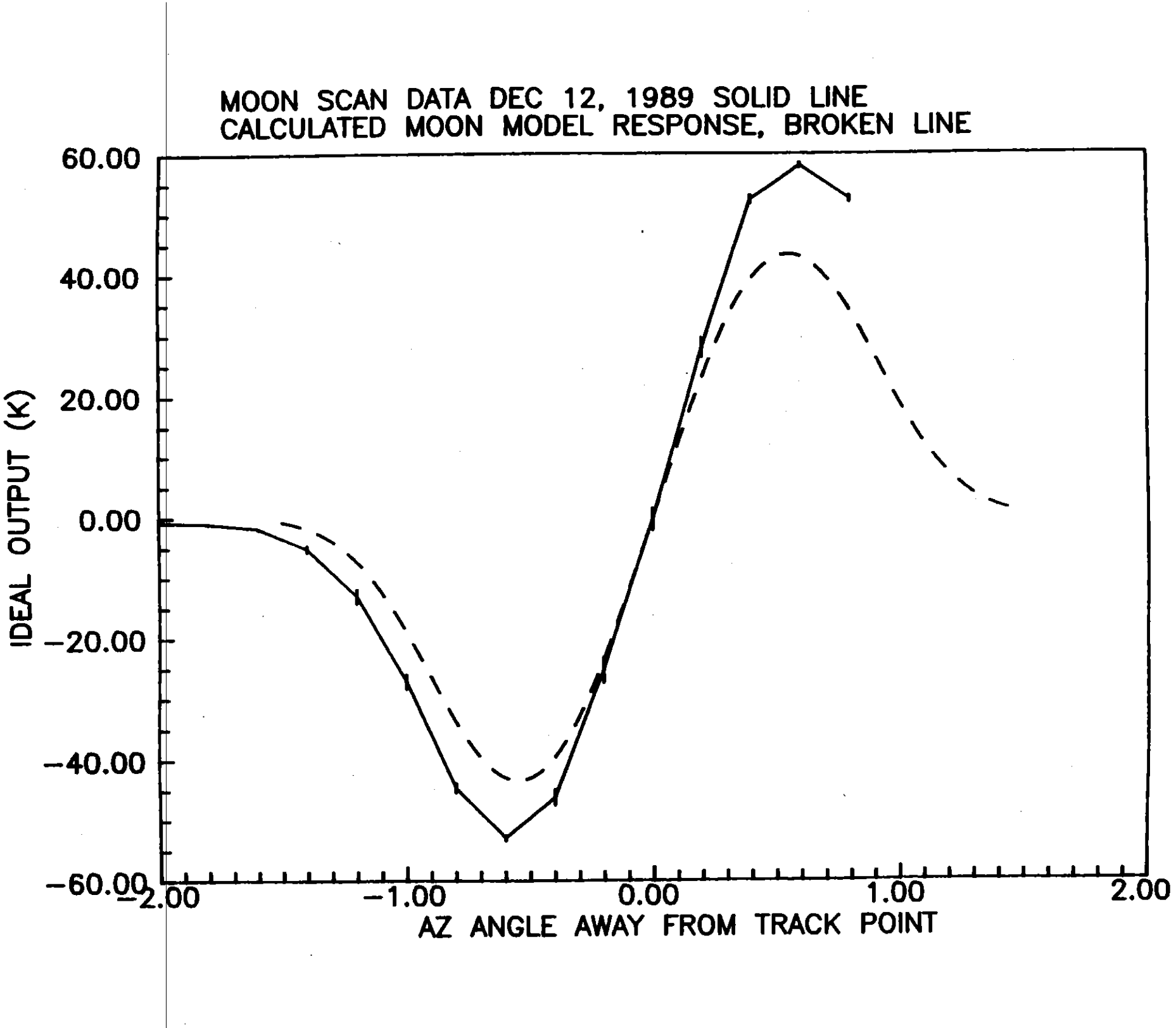
MOON SCAN DATA DEC 12, 1989 SOLID LINE
CALCULATED MOON MODEL RESPONSE, BROKEN LINE
60.00
40.00
20.00
0.00
-20.00
-40.00
-60.00
IDEAL OUTPUT (K)
-2.00
-1.00
0.00
1.00
2.00
AZ ANGLE AWAY FROM TRACK POINT

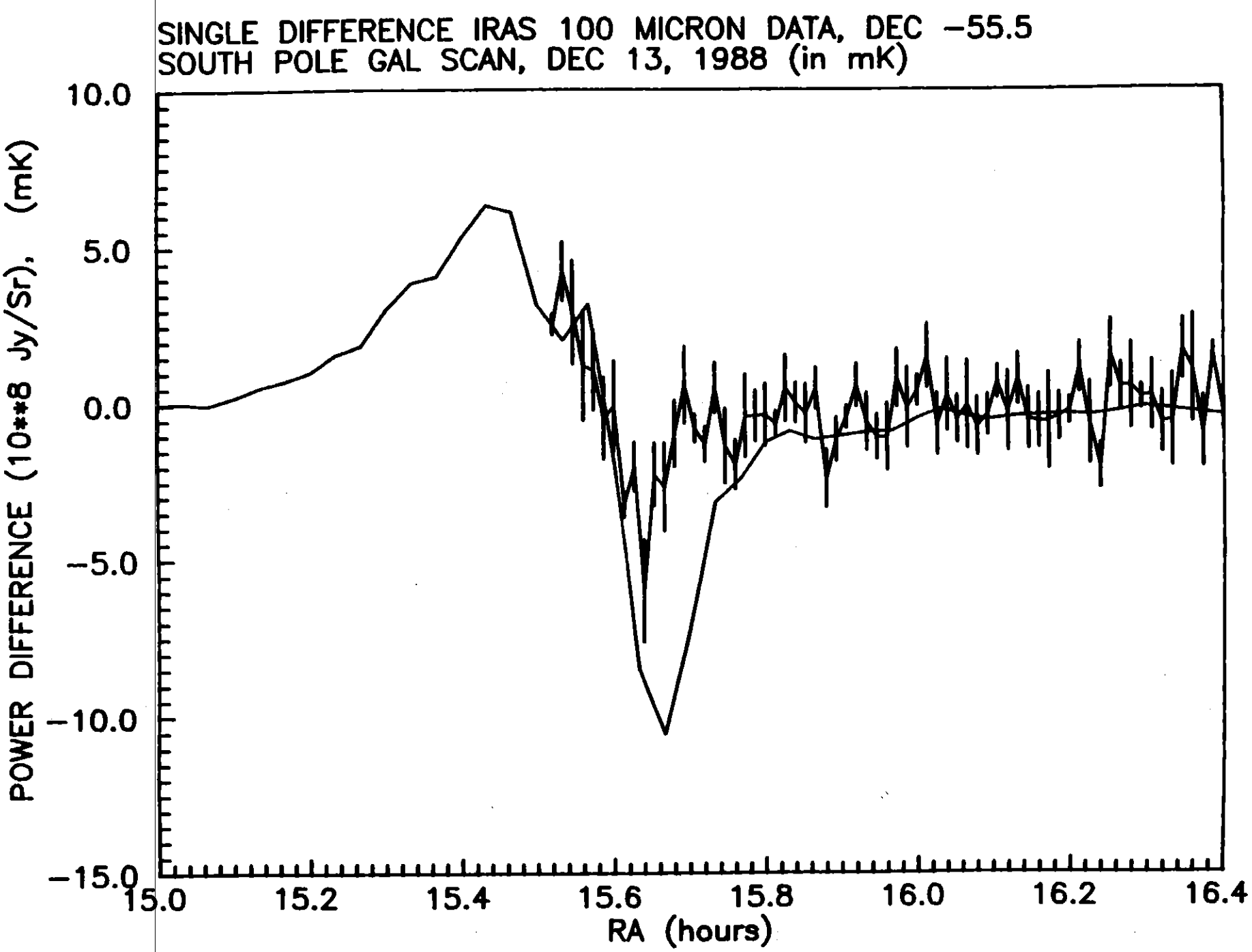
SINGLE DIFFERENCE IRAS 100 MICRON DATA, DEC −55.5
SOUTH POLE GAL SCAN, DEC 13, 1988 (in mK)
POWER DIFFERENCE (10**8 Jy/Sr), (mK)
10.0
5.0
0.0
−5.0
−10.0
−15.0
15.0
15.2
15.4
15.6
15.8
16.0
16.2
16.4
RA (hours)

IRAS 100 micron 2 x 2 DEGREE MAP. CELESTIAL COORDINATES

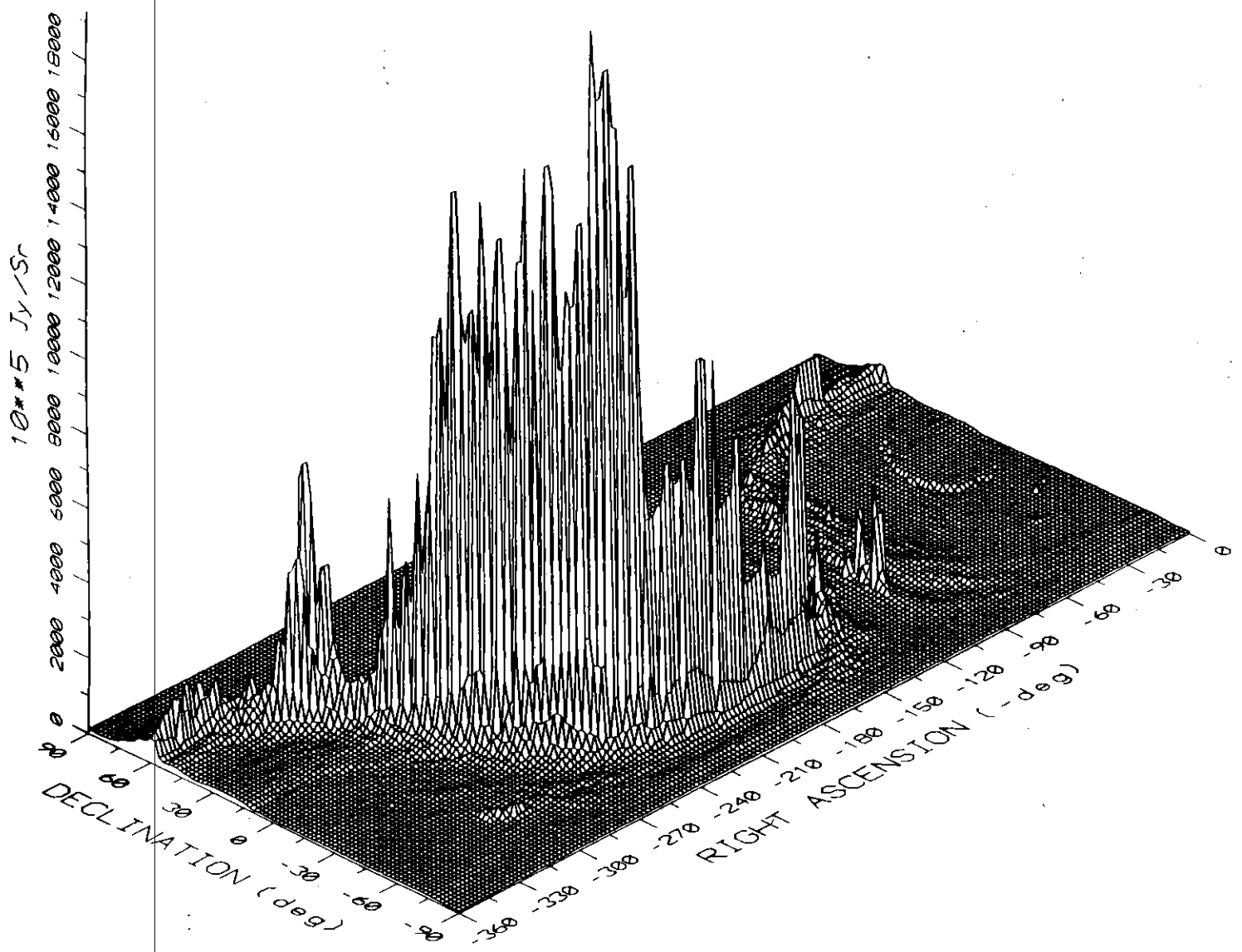

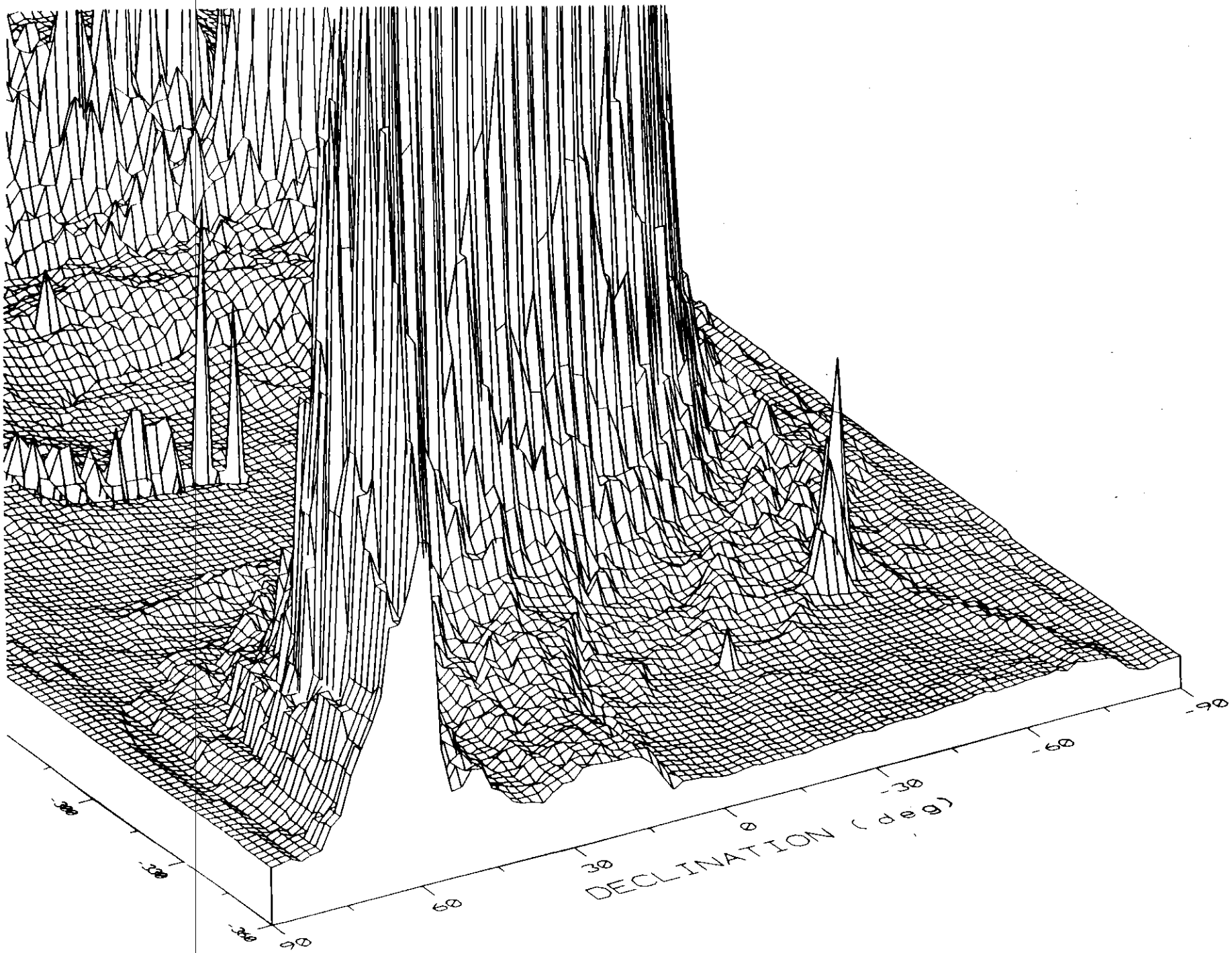
-90
-60
-30
0
30
60
90
DECLINATION (deg)

IRAS 100 micron .5 × .5 DEG MAP, MEASUREMENT REGION

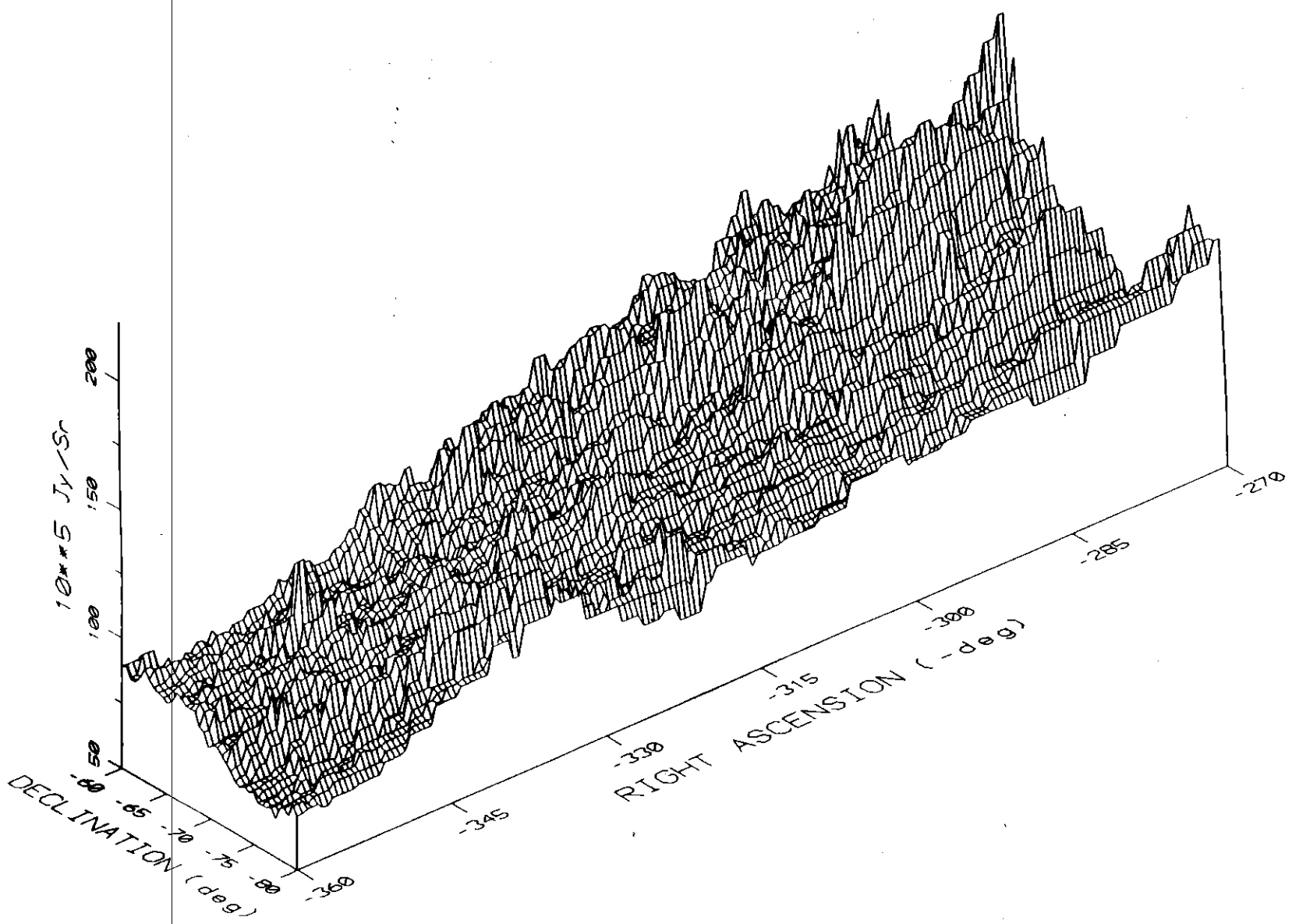

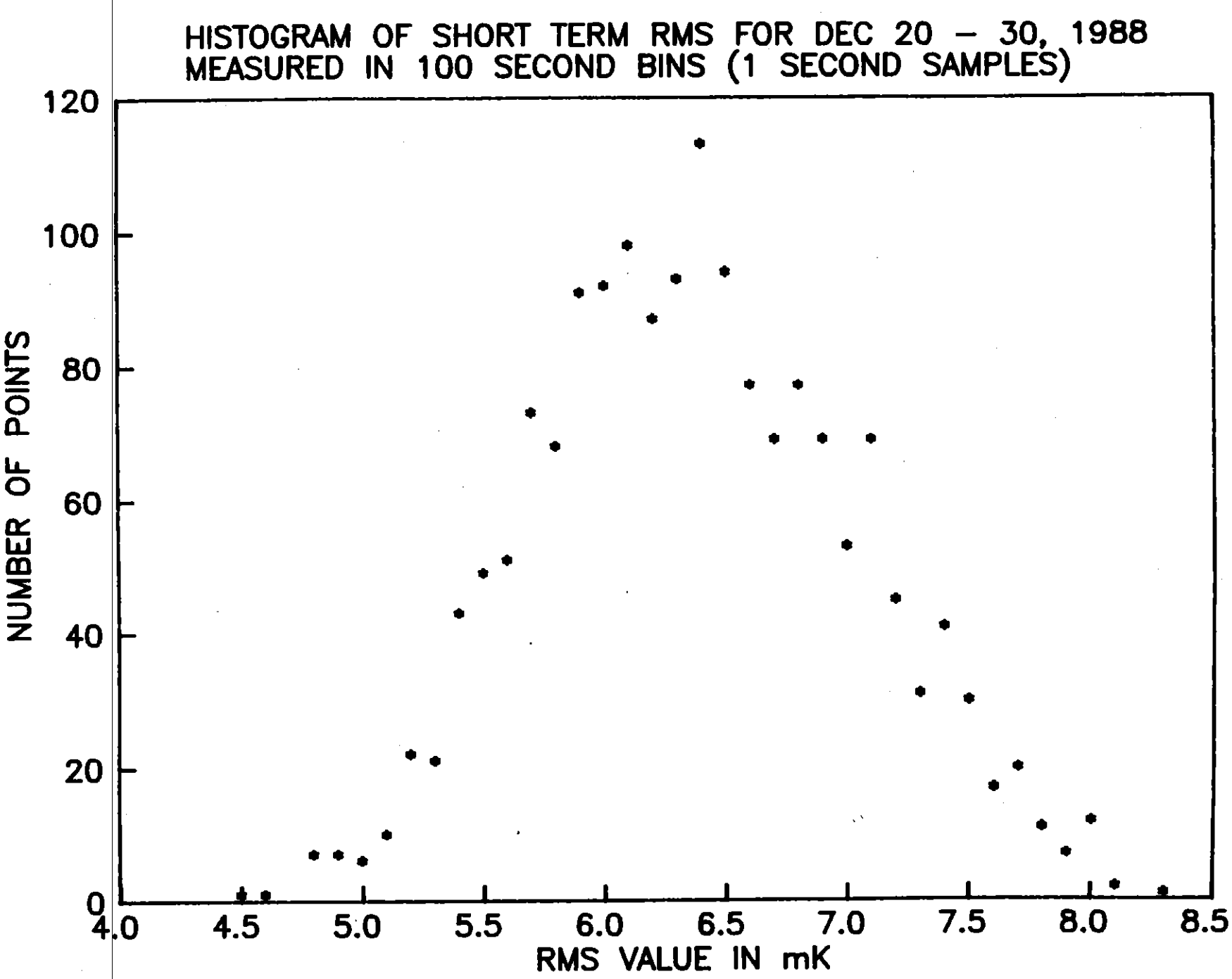
HISTOGRAM OF SHORT TERM RMS FOR DEC 20 – 30, 1988
MEASURED IN 100 SECOND BINS (1 SECOND SAMPLES)
NUMBER OF POINTS
0
20
40
60
80
100
120
4.0
4.5
5.0
5.5
6.0
6.5
7.0
7.5
8.0
8.5
RMS VALUE IN mK

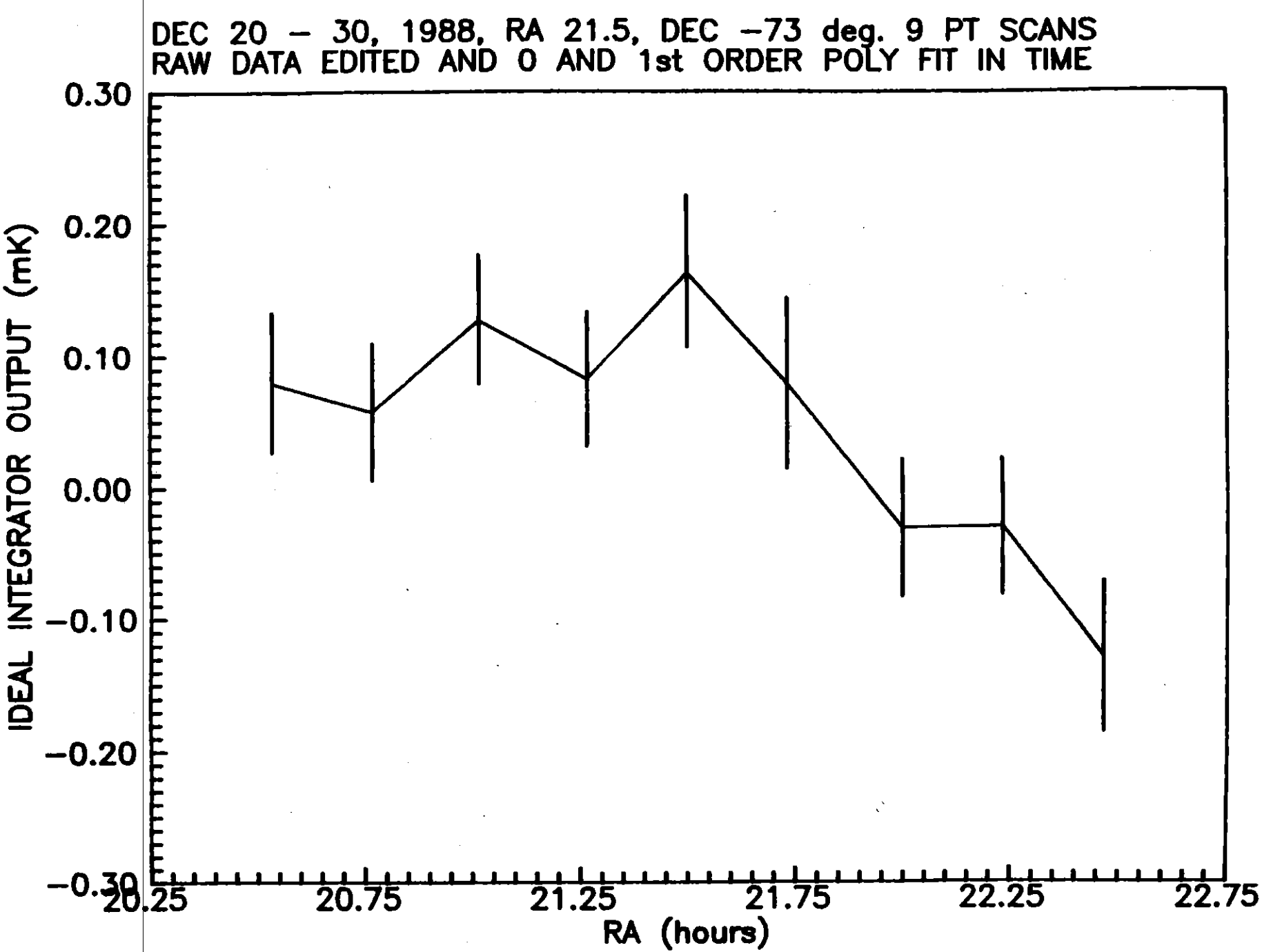
DEC 20 – 30, 1988, RA 21.5, DEC –73 deg. 9 PT SCANS
RAW DATA EDITED AND 0 AND 1st ORDER POLY FIT IN TIME
IDEAL INTEGRATOR OUTPUT (mK)
0.30
0.20
0.10
0.00
–0.10
–0.20
–0.30
20.25
20.75
21.25
21.75
22.25
22.75
RA (hours)

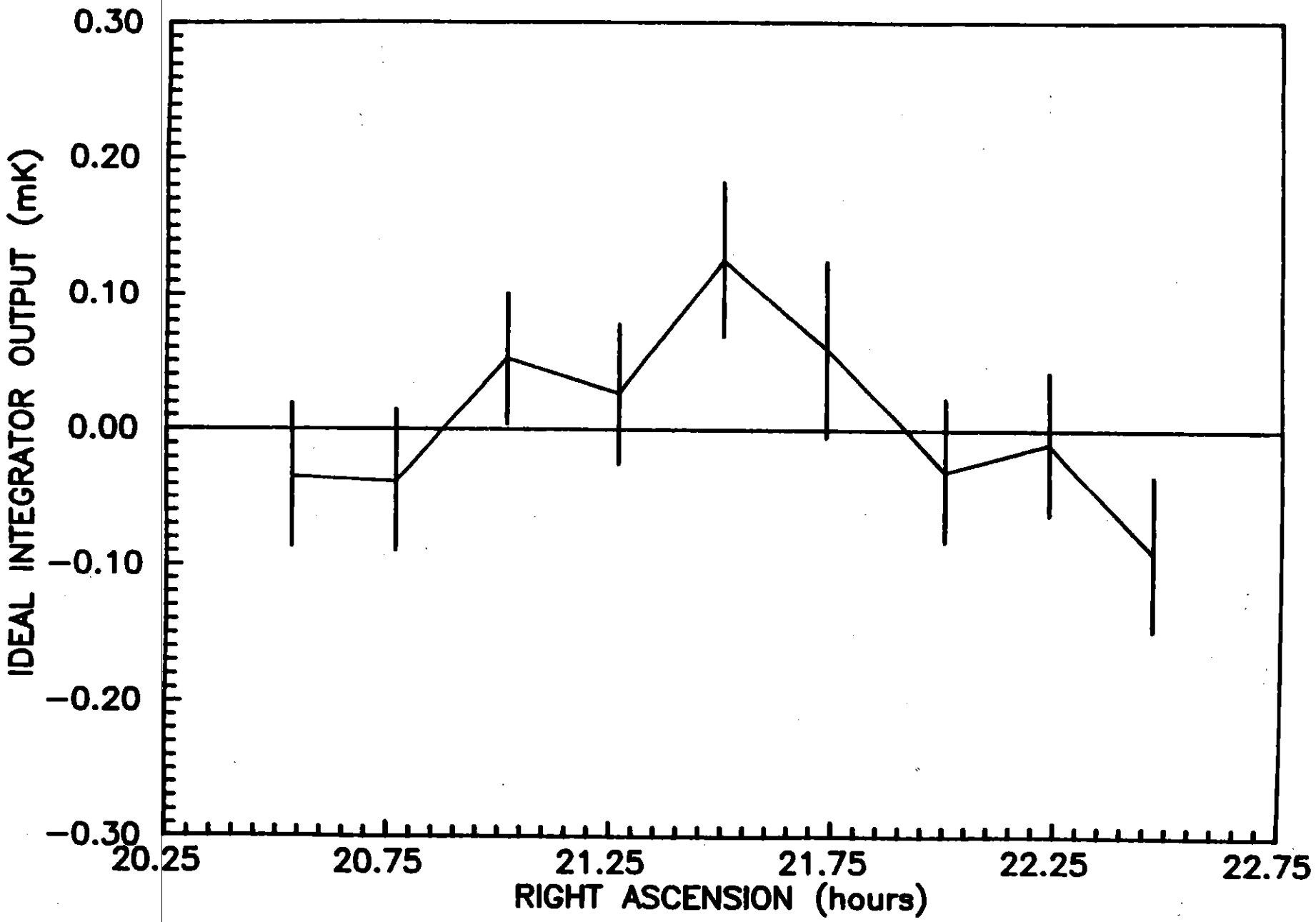
DEC 20–30, 1988 RA 20.5, DEC –73 deg 9 PT SCANS
LINEAR FIT IN RA REMOVED
IDEAL INTEGRATOR OUTPUT (mK)
0.30
0.20
0.10
0.00
–0.10
–0.20
–0.30
20.25
20.75
21.25
21.75
22.25
22.75
RIGHT ASCENSION (hours)